RSC Advances

Journal Name

RSC Advances

ARTICLE TYPE

Facile Construction Hybrid Polystyrene with a String of Lanterns Shape from Monovinyl–substituted POSS and Commercial Polystyrene *via* Friedel–Crafts Reaction and Its Properties

Liguo Li and Hongzhi Liu*

Hybrid polystyrene was easily prepared from monovinyl–substituted POSS and commercial polystyrene (PS) *via* the straightforward Friedel–Crafts reaction. The resulting hybrid polystyrene was thoroughly investigated by a series of characterization methods, such as FTIR, NMR, XRD, SAXS, DLS, POM,
10 DSC, TGA, SEM, TEM and an Abbe refractometer. Results showed that POSS were well dispersed in the polystyrene matrix at a nearly molecular level and no macrophase separation was observed; these hybrid polystyrenes exhibited different properties from pristine polystyrene, for example, solubility, crystalline and thermal properties *etc.*. Considering the strong aggregation tendency of POSS in nonsolvents, it was interesting to study the self–assembly behaviors of these hybrid polystyrenes modified by POSS. The
15 morphology of these hybrid polystyrenes in ethanol was investigated by dynamic lighting scattering, transmission electron microscopy. The studies illustrated that these hybrid polystyrenes could self–assemble into a series of spheres in ethanol; the diameters of these spheres decreased with increasing POSS loading.

Introduction

20 In the past few years, polyhedral oligomeric silsesquioxane (POSS)–based hybrid polymers have grown rapidly since POSS cages impart a wide range of improved thermal, mechanical, and physical properties to the parent polymer.[1–4] POSS can be incorporated into polymer matrix in different approach depending
25 on the type of organic substituent. Nonreactive organic substituents can enhance the compatibility of POSS with the polymer, thus preparing hybrid materials nanoreinforced by POSS *via* physical blending.[5,6] Reactive organic substituents can potentially enable POSS to be chemically incorporated into the
30 polymer matrix.[7,8] The chemical reactivity and self–assembly properties of POSS make it feasible to realize nanostructured materials with different architecture *via* a classical bottom–up approach.

Octavinyl functionalized POSS monomers are easily obtained
35 and have been explored as versatile precursors to prepare numerous novel molecules and hybrid materials. For example, it has been used to prepare some hybrid porous materials *via* free radical polymerization, Heck reaction and Freidel–Crafts reaction, *etc*.[9–14] In addition, octavinyl POSS was also employed
40 to modify traditional polymers, such as polyethylene glycol, polymethylacrylate, silicone rubber and so on.[15–18] By contrast, the introduction of monovinyl substituted POSS into polymer matrix is less reported by far.

Polystyrene is a general polymer and has been widely used in
45 various aspects for its well–known properties: easy to process and

functionalize, soluble in a broad range of solvents, outstanding thermal stability, and mild substrate as supporter.[19–21] POSS cages have been incorporated into polystyrene in various ways, including ATRP, RAFT, anion polymerization *etc.* to form hybrid
50 polystyrenes of various molecular architectures.[22–26] Starting from commercial polystyrene–butadiene–polystyrene (SBS), a novel hybrid organic/inorganic triblock copolymer with pendent polyhedral oligomeric silsesquioxane (POSS) molecules was also synthesized by a hydrosilation method.[27–28]

55 However, these reactions generally require noble metal catalysts and strict conditions and typically entail multiple procedures. Therefore, developing new strategies suitable for simple and relatively low–cost synthesis of these hybrid polymers modified by POSS is necessary. Friedel–Crafts alkylation
60 reaction has become an important method for assembling molecules and polymers because this reaction requires relatively mild conditions without any expensive catalyst, but achieves high efficiency. Reports have demonstrated that constructing hybrid polymers *via* Friedel–Crafts reaction is versatile and flexible and
65 allows economical and large–scale production of hybrid materials.[13]

Although the random copolymers of styrene and styryl–POSS were once prepared through radical copolymerization initiated by AIBN, it was difficult to control the molecular weight and
70 polydispersity of the resulting product.[29,30] In view of a large of phenyl groups in polystyrene, therefore, it is a practical route to prepare a series of POSS–based hybrid polystyrene *via* straight Friedel–Crafts reaction with monovinyl substituted POSS. Different from the previous random copolymerization method,

the molecular structure of the polystyrene backbone, including molecular weight and polydispersity, was defined prior to attaching POSS to the backbone. The introduction of POSS cages does not change the sequence and the degree of polymerization.

5 This provides us a unique opportunity to study the effect of POSS on polymer properties without introducing other effects that might arise from changes to the molecular structure of a host polymer.

These hybrid polystyrenes modified by POSS *via* the Friedel–

10 Crafts reaction have been thoroughly investigated by FTIR, NMR, XRD, DLS, POM, DSC, TGA and TEM. Solubility experiments showed that their solubility in ethanol can be tuned by varying POSS loading, which hinted that there probably existed self–assembly behaviors in ethanol. Although there are a

15 few papers on the self–assembly behaviors of POSS–containing hybrid polymers in aqueous solutions;[24,31] until now, there is no report on the self–assembly behaviors of POSS–based hybrid lantern polymers in ethanol media. Owing to the distinct size and geometry of the POSS cages and their exceptionally high

20 aggregation propensity, unique self–assembly behaviors are expected when POSS acts as hydrophilic group in this hybrid lantern polymer. The self–assembly behavior of this hybrid lantern polymer was investigated by transmission electron microscopy (TEM) and dynamic light scattering (DLS). In

25 addition, the refractive indices (RIs) of these hybrid polystyrenes based on POSS were also investigated.

Experimental

Materials

Polystyrene (M_w = 35000) were purchased from Aldrich.

30 Monovinyl substituted silsesquioxane (MVS) was prepared according to a previous report (Supporting Information).[32] Unless otherwise noted, all other reagents were obtained from commercial suppliers and used without further purification. CS_2 was purified using atmospheric distillation methods and stored

35 with 4 Å molecule sieves prior to use.

Characterization

FT–IR spectra were measured within a 4000 cm^{-1} to 400 cm^{-1} region on a Bruker TENSOR–27 infrared spectrophotometer (KBr pellet). ^{1}H NMR and ^{13}C NMR spectra were recorded in

40 CDCl$_3$ on a Bruker Avance–400 spectrometer without internal reference. The RIs were determined with an Abbe refractometer (WZS-I model, made in Shanghai, China) at 25 °C, with an accuracy of ±0.0001. TGA was performed on a Mettler Toledo TGA/DSC1 with heating rate of 10 °C/min from 30 °C to 800 °C

45 under N_2 (100 mL/min) at ambient pressure. DSC measurements were studied using SDTQ 600 of TA Instruments. The nanocomposites were loaded in aluminum pans, heated from 25 to 200 °C, then cooled to 25 °C, and finally reheated to 200 °C. The heating and cooling temperature ramping rates were

50 10 °C/min. The DSC data from the second heating cycle are reported in this paper. Powder X–ray diffraction (PXRD) were carried out on a Riguku D/MAX 2550 diffractometer with Cu–Kα radiation, 40 kV, 20 mA (λ = 1.542 Å) with the 2θ range of 5°~70° (scanning rate of 10°/min) at room temperature. SAXS

55 experiments were performed on Anton Par Saxes mc^2 with Cu Kα radiation at 40 kV/50 mA (λ = 1.5418 Å) at room temperature.

DLS measurements were performed on a multi–angle laser photometer equipped with a linearly polarized gallium arsenide (GaAs) laser (*k* = 658 nm; Wyatt Technology Co. DAWN

60 HELEOS). The measurements were conducted at a scattering angle of 99°. Field emission scanning electron microscopy (FE–SEM) tests were performed with a Hitachi S–4800 high resolution SEM. The samples of self–assembly behaviors for TEM (HR–TEM) observation were prepared by spreading a drop

65 of aggregate THF solution on a copper grid coated with a carbon film followed by air drying at 25 °C before the measurement on a JEM–1011 (100 kV) electron microscopy and JEM–2100 (200 kV) electron microscope (JEOL, Japan).

Synthesis of hybrid polystyrenes with POSS

70 A series of hybrid polystyrenes with different POSS loading were prepared, *i.e.* 5, 10, 15 and 20 wt %; these hybrid polystyrenes are denoted as PS/POSS_5, PS/POSS_10, PS/POSS_15 and PS/POSS_20, respectively. A typical procedure using PS/POSS_5 as the example: PS (1.0 g), anhydrous AlCl$_3$ (0.2 g,

75 1.5 mmol), MVS (0.05 g) and CS$_2$ (10 ml) were charged in an oven–dried flask (25 ml). The resulting mixture was vigorously stirred at room temperature for 0.5 h and refluxed at 45 °C for 24 h. After the mixture was cooled to room temperature, the mixture was added into 100 mL methanol drop by drop. The precipitates

80 were filtered and washed with methanol and then dried in vacuum at 50 °C for 24 h to obtain slightly yellow powders.

PS/POSS_5 was afforded as a slightly yellow powder (0.69 g, ca. 65 %). Elemental analysis calc. (wt. %) for C$_{1326}$H$_{1362}$O$_{12}$Si$_8$ or PS$_1$POSS$_{0.05}$: C 89.95, H 7.70; Found C 90.14, H 7.31.

85 PS/POSS_10 was afforded as a slightly yellow powder (0.92 g, ca. 84 %). Elemental analysis calc. (wt. %) for C$_{1356}$H$_{1422}$O$_{24}$Si$_{16}$ or PS$_1$POSS$_{0.10}$: C 87.80, H 7.70; Found C 88.44, H 7.27.

PS/POSS_15 was afforded as a slightly yellow powder (0.97 g, ca. 84 %). Elemental analysis calc. (wt. %) for C$_{1386}$H$_{1482}$O$_{36}$Si$_{24}$

90 or PS$_1$POSS$_{0.15}$: C 85.85, H 7.71; Found C 87.89, H 7.35.

PS/POSS_20 was afforded as a slightly yellow powder (0.98 g, ca. 82 %). Elemental analysis calc. (wt. %) for C$_{1416}$H$_{1542}$O$_{48}$Si$_{32}$ or PS$_1$POSS$_{0.20}$: C 83.97, H 7.72; Found C 86.36, H 7.39.
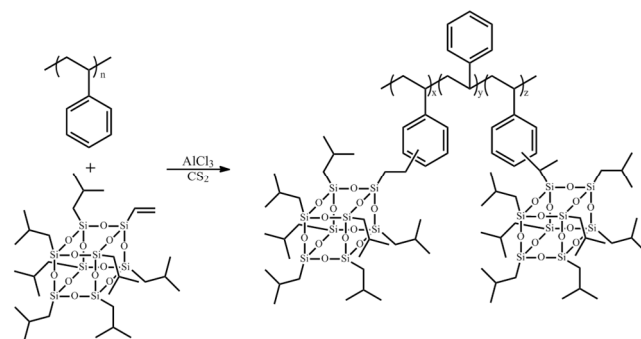
95 **Scheme 1**   Synthesis of PS/POSS nanocomposites.

Results and Discussion

Synthesis of hybrid polystyrene with POSS

As shown in Scheme 1, hybrid polystyrenes (PS) with POSS were synthesized through the Friedel–Crafts reaction of PS with

100 stoichiometric MVS in CS$_2$ at 45 °C for 24 h. Then the products were precipitated in methanol and filtered, finally dried in

vacuum at 50 °C for 24 h. The resulting materials were slightly yellow powders and they were soluble in most common solvents. In the Friedel-Crafts reaction, all the raw materials were dried or distilled prior to use; however, there still existed traces of water in raw materials such as PS, MVS or CS_2. The presence of traces of water actually initiated the protonation and the formation of carbocation, which promoted Friedel-Crafts reaction. Considering large amount of phenyl groups in polystyrene, a series of hybrid polystyrene with different weight ratios of MVS and polystyrene were designed and synthesized. In view of steric hindrance of POSS, we supposed that a phenyl group only reacted with one POSS; thus, the weight ratio of POSS increased from 5 to 20 % (5, 10, 15, 20 wt %), the molar ratio of POSS and phenyl groups corresponded to 1/162, 1/81, 1/54 and 1/40, respectively. The content of carbon and hydrogen in PS/POSS_5 to PS/POSS_20 was confirmed by elemental analysis. Energy dispersive X–ray spectrometry (EDX) further demonstrated that silicon content increased from PS/POSS_5 to PS/POSS_20 with increasing MVS content (Fig. S1†); although EDX was not quantitative, as an adjunctive means, it might reflect the relative content of silicon in the resulted hybrid composites to some degree.
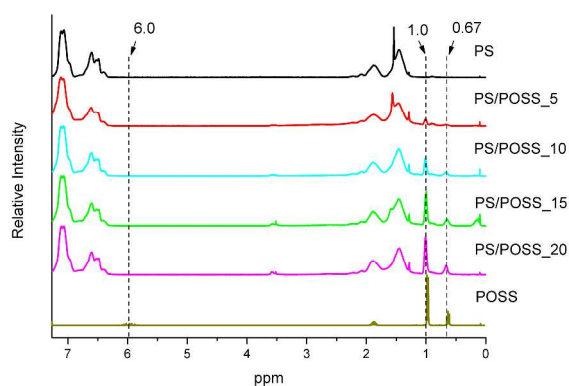
Fig. 1 H NMR spectra of PS, POSS and PS/POSS nanocomposites.

The resulting products were subjected to spectroscopic measurements. In the ^{1}H NMR spectra (Fig. 1), it was obviously observed that the characteristic signal of vinyl group of MVS at near 6.0 ppm disappeared in the PS/POSS nanocomposites, indicating that Friedel–Crafts reaction was complete. However, it was difficult to observe the signals of the new formation of two methylene, Si–C$\underline{H}_2$–C$\underline{H}_2$–, the signal of –C$\underline{H}_2$ linked with silicon atom was overlapped with the signal of –C$\underline{H}_3$ in the isobutyl group; another signal of –C$\underline{H}_2$ linked with phenyl group was broadened in the ^{1}H NMR spectra. In the process of Friedel–Crafts reaction, rearrangement probably occurred; however, it was impossible to identify the typical signals of the rearranged-product from proton NMR (*i.e.* Si–CH(CH$_3$)–) because of the overlap of the signals. Meanwhile, it can be obviously found that the characteristic signals of –C$\underline{H}_3$ and –C$\underline{H}_2$ in the isobutyl group emerged at 0.67 and 1.0 ppm, respectively and these two signals became stronger with the increase of POSS loading. In the ^{13}C NMR spectra of the hybrid polystyrene, it was observed that the signals of two carbons of vinyl group at 129.9 and 135.7 ppm

disappeared; however, the signal of carbon linked with silicon in the forming linker, *i.e.* Si–C$\underline{H}_2$–CH$_2$– was very weaker even after signal accumulation for 24 hours when the POSS loading was lower than 20 wt% (Fig. S2a†). This phenomenon hinted that F-C rearrangement probably occurred, *i.e.* the linker of -Si–CH(CH$_3$)– was formed, which was predominant. To better understand the reaction process and the chemical structure of the hybrid polystyrene, we prepared PS/POSS_100 nanocomposite, *i.e.* 100 wt % POSS as a model polymer. In the ^{13}C NMR spectrum of PS/POSS_100, it could be observed that four new signals appeared at 29.90, 29.00, 28.50 and 14.50 ppm, respectively, corresponding to the four carbon atoms in the linker units of Si–CH$_2$–CH$_2$– and Si–CH(CH$_3$)– formed between POSS and polystyrene, which demonstrated that rearrangement occurred in the Friedel–Crafts reaction (Fig. S2b and 2c†).[13]

Considering the overlap of the absorption band of vinyl group (1600 cm^{-1}) and phenyl groups, it was difficult to judge whether the Friedel–Crafts reaction between polystyrene and MVS occurred or not just from FTIR (Fig. 2). However, it was still observed a strong band at 1104 cm^{-1} in these hybrid polystyrene and the intensity increased gradually with the increase of POSS loading. This band was ascribed to the –Si–O–Si– stretching vibrations, which at least proved that the existence of POSS cages in these hybrid polystyrenes.
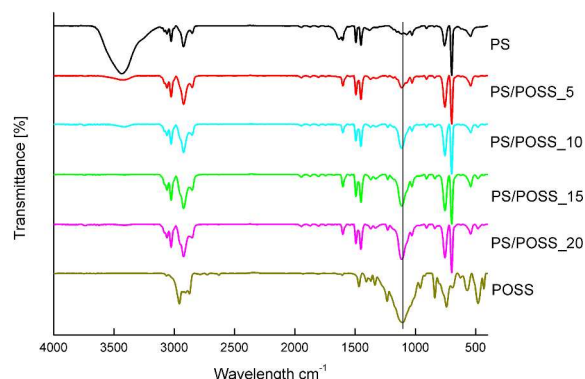
Fig. 2 FT–IR spectra of PS, POSS and PS/POSS nanocomposites.

Morphology properties of the hybrid nanocomposites

The crystallographic order of PS, POSS and PS/POSS nanocomposites were investigated by powder X–ray diffraction (PXRD) patterns. PXRD results (Fig. 3) showed that monovinyl substituted POSS was a highly crystalline solid and existed several sharp and strong peaks at 2θ = 8.5 , 11.5 , 19.6 and 20. It was observed that pure polystyrene had a broad amorphous peak at $2\theta \approx 20$ °, indicating that it was amorphous. All the hybrid polystyrenes exhibited a broad amorphous peak at $2\theta \approx 20°$ in the PXRD patterns, corresponding to the amorphous polystyrene matrix peak.[29] This meant that POSS was homogeneously distributed throughout polystyrene matrix. However, in contrast to the typical amorphous polymers, there existed one weak peak at $2\theta \approx 8°$ and the intensity of this peak gradually increased with the increase POSS loading. This fact would mean that POSS cages maintain a relevant self–assembling ability even when copolymerized by a predominantly statistical process, with the

formation of nanocrystal phases, possessing local long range order although the degree of the order is not very high.[33,34]
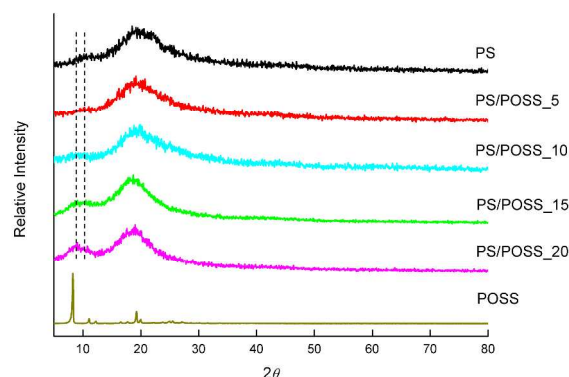
Fig. 3 PXRD figures of PS, POSS and PS/POSS nanocomposites.

5 To further investigate the crystallinity of these composites, polarized optical microscopy (POM) was also performed. POM graphs showed that some crystals existed in the polystyrene matrix (Fig. S3†) and with the increase POSS loading, the crystal regions expanded. This finding suggested that certain
10 nanocrystallines existed in the nanocomposites which was in accordance with PXRD.

SAXS was also used to investigate the morphologies of these hybrid nancomposites. The SAXS patterns showed that no obvious peaks could be seen in PS and PS/POSS nanocomposites,
15 implying the amorphous structure were dominant in hybrid nanocomposites (Fig. S4†). The MVS possessed an apparent maximum at q=5.9 nm^{-1}, which vanished in the PS/POSS nanocomposites, demonstrating that the POSS was well–distributed in PS matrix without large–scale aggregation.[35,36] The
20 SAXS results were consistent with XRD analysis, further confirming that POSS was homogeneously dispersed in the PS matrix, at least macrophase separation did not occur.
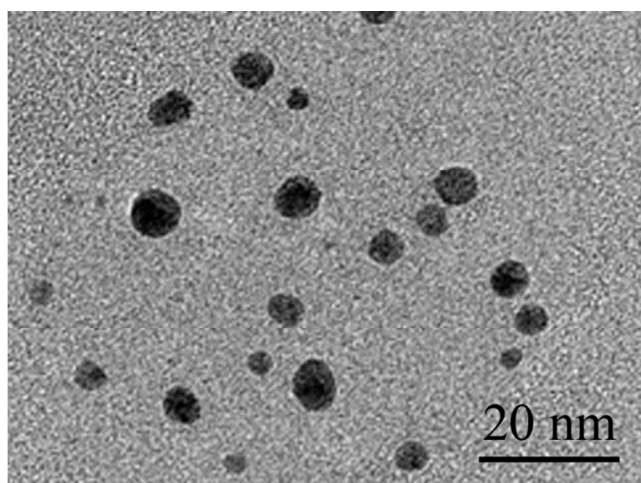
Fig. 4 HR–TEM image of PS/POSS_15.

25 To further elucidate the microstructure of the lantern shaped polymers, we made direct observations of selected samples using transmission high–resolution transmission electron microscopy (HR–TEM). A drop of hybrid polystyrene THF solution was spreaded on a copper grid coated with a carbon film followed by
30 air drying at 25 °C before the measurement. Interestingly, the HR–TEM image of hybrid polystyrene with 15 wt % of grafting POSS showed a well–dispersed organization of small–sized self–assembly behavior, and self–aggregate part with average diameter of around 5 nm (Fig. 4), which was similar to the report on PS–
35 POSS copolymers.[37] We infer that POSS cages pendent along the polystyrene chain are well–dispersed in the polystyrene matrix at a molecular level and there is no obvious aggregation of POSS cages, consistent with our WAXD and SAXS observations described above.

40 **Self–assembly behaviors of these hybrid polystyrenes in ethanol**

Polystyrene and POSS/PS nanocomposites did not dissolve in ethanol; however, the dissolvability of hybrid polystyrene could be improved and became better and better with increasing POSS
45 loading even if a small amount of THF was added to ethanol. This should be ascribed to the alteration of the solubility parameter of polystyrene by the incorporation of POSS, which was surrounded by seven aliphatic isobutyl groups. This phenomenon hinted that these polystyrene modified by POSS
50 could probably exhibit different self–assembly behaviors in this selective solvent, *i.e.* ethanol. Indeed, the self–assembly behaviors of these hybrid polystyrenes were observed by TEM and DLS when a solution of PS/POSS in THF was added to a large amount of ethanol. From TEM image, it was interesting to
55 find that pure polystyrene formed discrete spheres with a uniform size about 500 nm for its bad solubility in ethanol (Fig. S5†). For these hybrid polystyrenes modified by POSS, they could also self–assembled into spheres and the sizes of these hybrid polystyrenes decreased with the increase of POSS content.
60 However, these spheres were not all discrete and some of them interconnected together in the TEM images; the interconnection became more and more serious with increasing POSS loading (Fig. 5). The driving force for this interconnection was the solvent evaporation during the TEM sample preparation, which
65 led to aggregation of POSS cages.
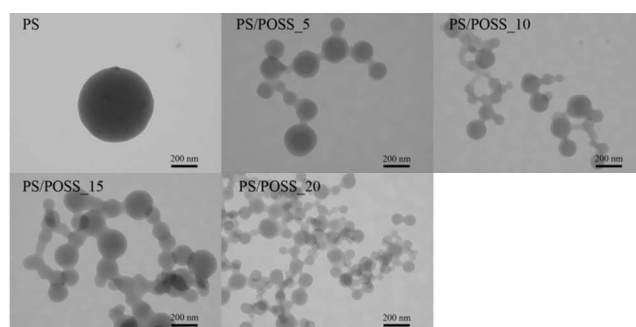
Fig. 5 TEM images of PS and PS/POSS nanocomposites.

To better understand the mechanism of the self–assembly process of these hybrid polystyrene, a schematic diagram was
70 suggested in Scheme 2. After POSS were grafted onto PS chain *via* the Friedel–Crafts reaction, hybrid polystyrenes with a string of lanterns shape were obtained. When these hybrid nanocomposites were dissolved in THF, the chains were in chaotic state. As soon as the composites were transferred into
75 ethanol, the hydrophobic PS chains aggregated to form a core;

while the hydrophilic POSS were distributed on the surface of the core acting as the hydrophilic "corona". The difference of the solubility of PS segment and POSS drove the PS/POSS nanocomposites to form solid spheres like "corona" structure.

5　　To clarify the important role of POSS in the self–assembly behaviors of these hybrid polystyrenes in ethanol, we also investigated morphology of these hybrid polystyrenes in ethanol *via* light scattering. The DLS results indicated that the statistical hydrodynamic diameter of the hybrid nanocomposites reduced

10 with the increase of POSS with the increase of POSS content, demonstrating that the existence of POSS could reduce the diameter of the spheres; the more POSS, the smaller diameter of spheres was formed (Fig. S6†). The introduction of more POSS into polystyrene matrix could lead to better solubility in ethanol.

15 Only by reducing the size of spheres could enlarge the specific surface area, more hydrophilic groups could exist on the periphery of PS core. Consequently, the statistical size decreased with the increase of POSS loading.
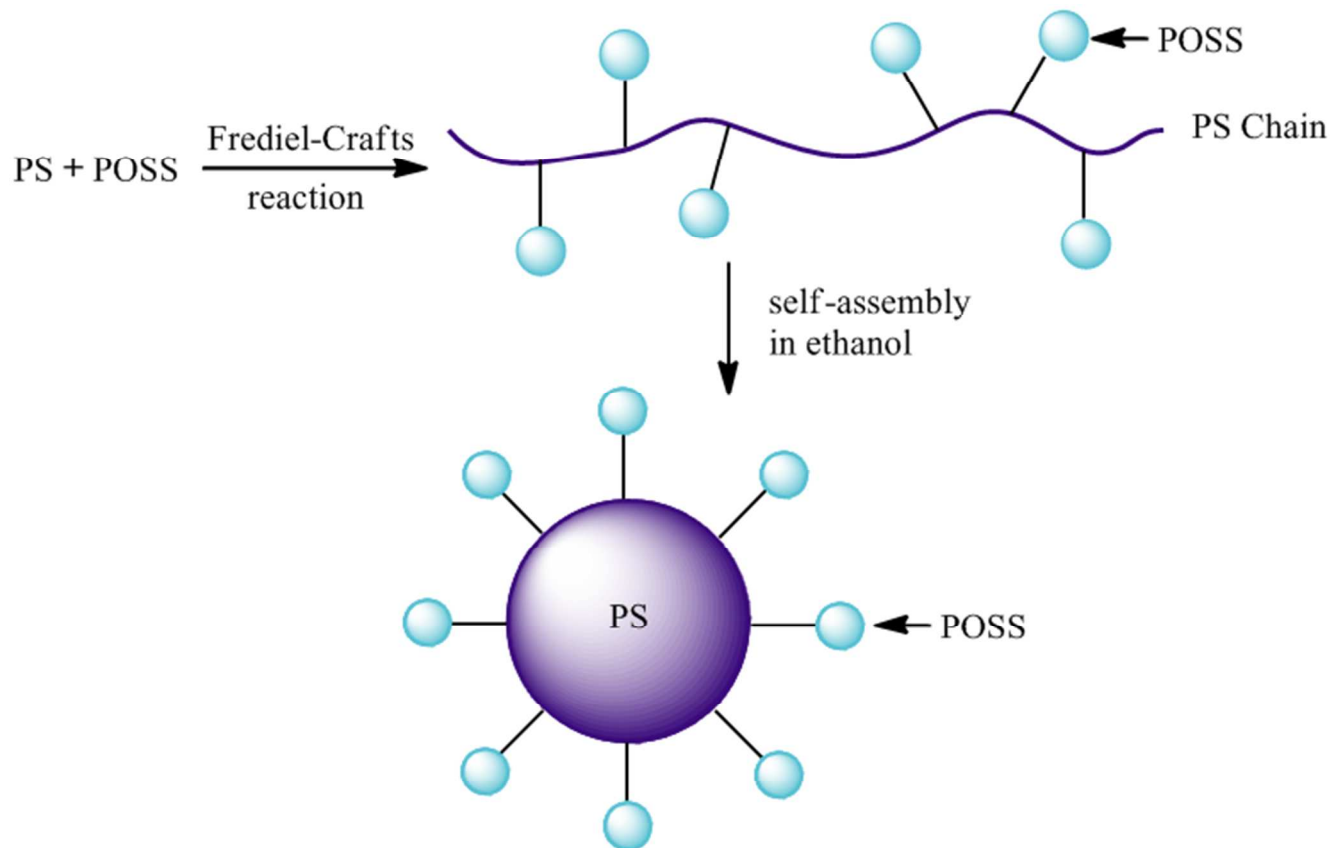
20　　　　　　　　　　　　**Scheme 2**　　A proposed working mechanism of PS/POSS sphere formation in ethanol.

Wettability of these polystyrene films

The wettability of the as–prepared hybrid nanocomposites was evaluated by the water contact angle (CA) measurement. Polystyrene is a hydrophobic material with a water CA of

25 $96.5°$.[38,39] It was interesting to observe that the water CA increased to approximately $99°$ after the incorporation of 5 % wt POSS into polystyrene; with further increasing POSS loading, the water CA almost remained invariable, (as shown in Fig. S7† and Fig. S8†). This implied that the POSS nanostructures were

30 preferentially oriented air–side when POSS loading was lower; and the polystyrene surface was nearly covered with POSS when POSS loading reached certain content. Thus, the water CA did not increase even if further increased POSS loading.[40]

Thermodynamical features

35 The glass transition behavior of pure PS and PS/POSS nanocomposites are described by DSC thermogram in Fig. 6. It could be seen that whether PS or hybrid PS with POSS displayed single glass transition temperatures. The pure PS exhibits an

endotherm approximately at 80 °C, corresponding to the T_g of

40 pure PS and the enhancement of T_g transition of the PS/POSS hybrid composites is obviously to be found in Fig. 6. This suggests that the POSS, especially the inorganic silica cores, accumulate heat enough to transfer the glass transition upward.[2,41–43] Moreover, the T_g of PS/POSS nanocomposites

45 became inconspicuous with the further increase of POSS loading. The incorporation of POSS cages into polystyrene matrix would increase both free volume and steric hindrance of the polystyrene matrix. More free volume would lead to lower T_g; however the increasing steric hindrance would lead to higher T_g , the final T_g

50 was a result of comprehensive factors.
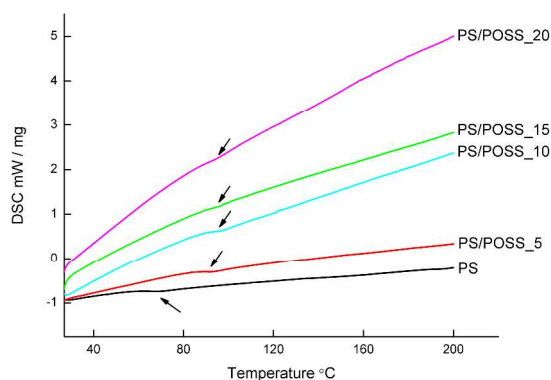
Fig. 6   DSC thermograms of PS and PS/POSS nanocomposites.
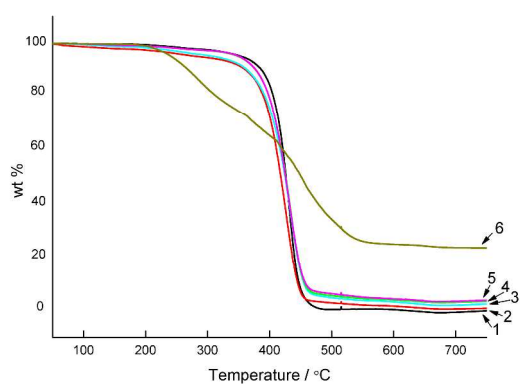
Fig. 7   Thermal gravimetric analysis of PS, POSS and PS/POSS
5 nanocomposites (1. PS; 2. PS/POSS_5; 3. PS/POSS_10; 4. PS/POSS_15;
5. PS/POSS_20, 6. POSS).

The thermal stabilities of PS/POSS nanocomposites were determined by thermal gravimetric analysis (TGA) under N_2 at 10 °C min^{-1} (Fig. 7). PS/POSS nanocomposites exhibited high
10 thermal decomposition temperatures (T_d at 5 wt %) at most up to 350 °C, which were higher than that of MVS, but lower than that of PS. The initial thermal decomposition of POSS started from organic substituents; the thermal stability of vinyl group and isobutyl groups were lower than that of phenyl groups, thus
15 leading to lower T_d. Within the experimental temperature range, the TGA curves of all the PS/POSS nanocomposites displayed similar degradation profiles, *i.e.*, only one main degradation step could be obviously observed in the TGA curves, which suggested that the existence of the POSS did not significantly affect the
20 degradation mechanism of the PS matrix. The introduction of POSS into the PS matrix showed a significant effect on improving the thermal stability, resulting in a tardy weight loss rate and an enhanced char yield in the higher temperature region. This effect was observed to be increasingly significant with the
25 concentration of POSS cages increase. The higher char yields for PS/POSS nanocomposites implied that there were fewer volatiles being released from the nanocomposites during heating. The decreased rate of volatile release from the hybrid composites suggested the improved flame retardance.[8]

30 **Optical properties**

POSS as fillers to modify the refractive indices (RIs) of polymer films *via* physical blending have been studied.[44-46] The polymer films exhibited lower RIs with the addition of POSS fillers and the RIs decreased with the increasing POSS loading. Hence, we
35 expected that we could tune the *n* value of RI by controlling the POSS loading in the PS/POSS nanocomposites *via* chemical grafting. We prepared thin films cast from the THF solutions of the PS/POSS nanocomposites. The PS/POSS nanocomposites (10 mg) were dissolved in 1 ml THF solution, followed by casting
40 onto the surface of illuminating prism. After 1 h at ambient temperature and 1 h at 80 °C, PS/POSS nanocomposite thin films were obtained. The *n* values were determined using an Abbe refractometer at 25 °C. RIs of the composite films with variable concentrations of POSS were measured for five times and the
45 averages of the values were shown in Fig. 8. As we expected, the *n* values decreased in the range from 1.6050 to 1.5940 by increasing POSS loading (Fig. 8). The RIs of nanocomposite films with POSS were lower than that of pure PS; moreover, the RIs of composites decreased almost linearly with the increase of
50 POSS content. These results suggested that the introduction of POSS could lower the RIs of PS films and the RI can be quantitatively tuned by changing POSS loading in PS *via* chemical grafting. The mechanism of lowering of refractivity can be explained that isobutyl groups on POSS can effectively create
55 the exclusion volumes. Consequently, the reduction of the packing of the PS chains likely occurs, resulting in the lowering refractivity. Therefore, PS/POSS nanocomposite films exhibited lower RIs than that of pure PS film. According to the previous reports, the degree of decrease in RIs by the introduction of POSS
60 was large enough for the application of the optical fibers.[46,47] Thus, the purpose for design of grafting POSS to polymers could be applicable in the practical materials.
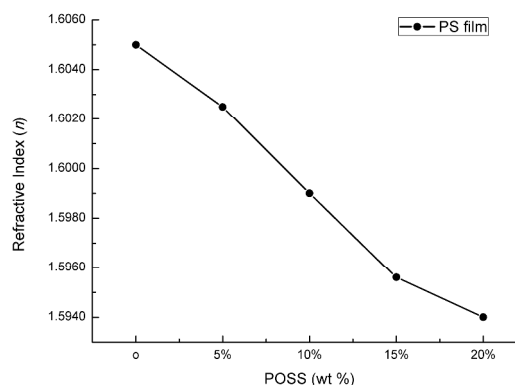
Fig. 8   RIs (*n*) of the PS/POSS nanocomposite films containing various
65   content of POSS.

Conclusions

In summary, a facile route to prepare hybrid polystyrene with POSS as pendent substituents was achieved *via* the Friedel–Crafts reaction of polystyrene with monovinyl substituted POSS. It was
70 interesting that these hybrid polystyrene nanocomposites exhibited a certain crystalline due to the introduction of intact POSS cages. These hybrid polystyrene nanocomposites had better solubility in ethanol than pristine polystyrene and could self–

assemble into spheres. The sizes of these formed spheres decreased with the increasing POSS loading.

The method in this paper represents an ideal approach to prepare new type of hybrid nanocomposites based on POSS and numerous hybrid polymer materials with novel properties based on POSS could be prepared in the future.

Acknowledgements

Notes and references

Key Laboratory of Special Functional Aggregated Materials, Ministry of Education, School of Chemistry and Chemical Engineering, Shandong University, Jinan 250100, P. R. China Tel: +86 531 88364691; E–mail: liuhongzhi@sdu.edu.cn

† Electronic Supplementary Information (ESI) available: EDX figures of PS and PS/POSS nanocomposites; ^{13}C NMR figure of PS/POSS_15; POM graphs of PS/POSS nanocomposites; SAXS figures of PS, POSS and PS/POSS nanocomposites; TEM graph of PS; DLS figures of PS and PS/POSS nanocomposites; CA figures of PS, POSS and PS/POSS nanocomposites; Optical graphs of PS/POSS nanocomposites membrane; SEM graphs of PS and PS/POSS nanocomposites. See DOI: 10.1039/b000000x/

1 G. Li, L. Wang, H. Ni and C. Pittman, *J. Inorg. Organomet. Polym.*, 2001, **11**, 123–154.

2 D. Cordes, P. Lickiss and F. Rataboul, *Chem. Rev.*, 2010, **110**, 2081–2173.

3 H. Liu, S. Kondo, N. Takeda and M. Unno, *J. Am. Chem. Soc.*, 2008, **130**, 10074–10075.

4 A. Romo–Uribe, P. Mather, T. Haddad and J. Lichtenhan, *J. Polym. Sci.; Part B: Polym. Phys.*, 1998, **36**, 1857–1872.

5 S. Kuo and F. Chang, *Prog. Polym. Sci.*, 2011, **36**, 1649–1696.

6 Y. Wu, L. Li, S. Feng and H. Liu, *Polym. Bull.*, 2013, **70**, 3261–3277.

7 J. Choi, J. Harcup, A. Yee, Q. Zhu and R. Laine, *J. Am. Chem. Soc.*, 2001, **123**, 11420–11430.

8 H. Liu and S. Zheng, *Macromol. Rapid Commun.*, 2005, **26**, 196–200.

9 I. Nischang, O. Brueggemann and I. Teasdale, *Angew. Chem. Int. Ed.*, 2011, **50**, 4592–4596.

10 F. Alves, P. Scholder and I. Nischang, *ACS Appl. Mater. Interfaces*, 2013, **5**, 2517–2526.

11 D. Wang, W. Yang, L. Li, X. Zhao, S. Feng and H. Liu, *J. Mater. Chem. A*, 2013, **1**, 13549–13558.

12 D. Wang, L. Xue, L. Li, B. Deng, S. Feng, H. Liu and X. Zhao, *Macromol. Rapid Commun.*, 2013, **34**, 861–866.

13 Y. Wu, D. Wang, L. Li, W. Yang, S. Feng and H. Liu, *J. Mater. Chem. A.*, 2014, **2**, 2160–2167.

14 W. Chaikittisilp, M. Kubo, T. Moteki, A. Sugawara–Narutaki, A. Shimojima and T. Okubo, *J. Am. Chem. Soc.*, 2011, **133**, 13832–13835.

15 D. Wang, S. Varanasi, E. Strounina, D. Hill, A. Symons, A. Whittaker and F. Rasoul, *Biomacromolecules*, 2014, **15**, 666–679.

16 B. Tan, H. Hussain and C. He, *Macromolecules*, 2011, **44**, 622–631.

17 K. Tanaka, S. Adachi and Y. Chujo, *J. Polym. Sci.; Part A: Polym. Chem.*, 2009, **47**, 5690–5697.

18 D. Chen, S. Yi, W. Wu, Y. Zhong, J. Liao, C. Huang and W. Shi, *Polymer*, 2010, **51**, 3867–3878.

19 B. Safadi, R. Andrews and E. Grulke, *J. Appl. Polym. Sci.*, 2002, **84**, 2660–2669.

20 R. Sen, B. Zhao, D. Perea, M. Itkis, H. Hu, J. Love, E. Bekyarova and R. Haddon, *Nano Letters*, 2004, **4**, 459–464.

21 S. Stankovich, D. Dikin, G. Dommett, K. Kohlhaas, E. Zimney, E. Stach, R. Piner, S. Nguyen and R. Ruoff, *Nature*, 2006, **442**, 282–286.

22 Z. Ge, D. Wang, Y. Zhou, H. Liu and S. Liu, *Macromolecules*, 2009, **42**, 2903–2910.

23 Y. Lin and S. Kuo, *Polym. Chem.*, 2012, **3**, 882–891.

24 W. Zhang, B. Fang, A. Walther and A. Muller, *Macromolecules*, 2009, **42**, 2563–2569.

25 Y. Deng, C. Yang, C. Yuan, Y. Xu, J. Bernard, L. Dai and J. Gerard, *J. Polym. Sci.; Part A: Polym. Chem.*, 2013, **51**, 4558–4564.

26 T. Hirai, M. Leolukman, S. Jin, R. Goseki, Y. Ishida, M. Kakimoto, T. Hayakawa, M. Ree and P. Gopalan, *Macromolecules*, 2009, **42**, 8835–8843.

27 D. Drazkowski, A. Lee, T. Haddad and D. Cookson, *Macromolecules*, 2006, **39**, 1854–1863.

28 B. Fu, A. Lee and T. Haddad, *Macromolecules*, 2004, **37**, 5211–5218.

29 J. Wu, T. Haddad, G. Kim and P. Mather, *Macromolecules*, 2007, **40**, 544–554.

30 H. Zhang, H. Lee, Y. Shin, K. Yoon, S. Noh and D. Lee, *Polym. Int.*, 2008, **57**, 1351–1356.

31 X. Yu, S. Zhong, X. Li, Y. Tu, S. Yang, R. Van Horn, C. Ni, D. Pochan, R. Quirk, C. Wesdemiotis, W. Zhang and S. Cheng, *J. Am. Chem. Soc.*, 2010, **132**, 16741–16744.

32 H. Liu, M. Puchberger and U. Schubert, *Chem. Eur. J.*, 2011, **17**, 5019–5023.

33 W. Chaikittisilp, A. Sugawara, A. Shimojima and T. Okubo, *Chem. Mater.*, 2010, **22**, 4841–4843.

34 M. Roll, J. Kampf, Y. Kim, E. Yi, R. Laine, *J. Am. Chem. Soc.*, 2010, **132**, 10171–10183.

35 L. Matejka, A. Strachota, J. Plestil, P. Whelan, M. Steinhart and M. Slouf, *Macromolecules*, 2004, **37**, 9449–9456.

36 J. Miao, L. Cui, H. Lau, P. Mather and L. Zhu, *Macromolecules*, 2007, **40**, 5460–5470.

37 M. Niu, T. Li, R. Xu, X. Gu, D. Yu and Y. Wu, *J. Appl. Polym. Sci.*, 2012, **129**, 1833–1844.

38 M. Jin, X. Feng, L. Feng, T. Sun, J. Zhai, T. Li and L. Jiang, *Adv. Mater.*, 2005, **17**, 1977–1981.

39 C. Extrand, *Langmuir*, 2003, **19**, 3793–3796.

40 S. Turri and M. Levi, *Macromolecules*, 2005, **38**, 5569–5574.

41 M. Noh and D. Lee, *Polym. Bull.*, 1999, **42**, 619–626.

42 B. Fu, L. Yang, R. Somani, S. Zong, B. Hsiao, S. Phillips, R. Blanski and P. Ruth, *J. Polym. Sci.; Part B: Polym. Phys.*, 2001, **39**, 2727–2739.

43 H. Xu, S. Kuo, J. Lee and F. Chang, *Polymer*, 2002, **43**, 5117–5124.

44 K. Tanaka, S. Adachi and Y. Chujo, *J. Polym. Sci., Part A: Polym. Chem.*, 2010, **48**, 5712-5717.

45 K. Tanaka, K. Inafuku, S. Adachi and Y. Chujo, *Macromolecules*, 2009, **42**, 3489–3492.

46 J. Jeon, K. Tanaka and Y. Chujo, *J. Polym. Sci., Part A: Polym. Chem.*, 2013, **51**, 3583-3589.

47 A. Evert, A. James, T. Hawkins, P. Foy, R. Stolen, P. Dragic, L. Dong, R. Rice and J. Ballato, *Opt. Express*, 2012, **20**, 17393–17401.